Effects of Cutouts on the Dynamic Response of Curved Rectangular Composite Panels

Garry J. Cyr,* Ronald L. Hinrichsen,† and Richard A. Walley‡
Air Force Institute of Technology, Wright-Patterson Air Force Base, Ohio

Numerical results obtained by the finite-element method were compared with experimental results obtained by holographic interferometry to quantify the effects of cutout size and orientation on the first five natural frequencies and mode shapes of a curved Gr-Ep panel. The clamped-clamped panels had a quasi-isotropic layup $[0, -45, 45, 90]_S$ and measured 12 in. (30.48 cm) high with a 12-in. (30.48-cm) chord. Cutouts having dimensions of 2×2 in. (5.08×5.08 cm), 2×4 in. (5.08×10.16 cm) and 4×4 in. (10.16×10.16 cm) were centrally located in the panels. The effects of the orientation of the 2×4 in. (5.08×10.16 cm) cutout were studied. When the finite-element results were compared with the time-averaged holograms, the two techniques showed close correlation of both the natural frequencies and mode shapes. Increasing the cutout size resulted in the expected reduction in natural frequency. An unexpected mode switch was observed to occur in the first two modes as more material was removed from the panel. It was found that the 0-deg cutout orientation had a significant effect on the panel stiffness, whereas the other cutout orientations did not significantly effect the stiffness.

Nomenclature

E_1 = Young's modulus in longitudinal fiber direction
E_2 = Young's modulus in the transverse fiber direction
G_{12} = shear modulus
K_{eq} = equivalent spring stiffness
m = mass
t = panel thickness
ν_{12}, ν_{21} = Poisson's ratios
ρ = mass density
ω = frequency

Introduction

THE USE of composite materials in aerospace vehicles has increased dramatically over the past decade and the prospect for its further and increased use is certain for many applications. The static response of these materials has been studied extensively and understanding has been gained to the point that designers feel confident in its use. Although the dynamic behavior of composites has been studied to some degree, questions still remain that must be answered so that this behavior can be predicted and confidence can be gained. In the area of aircraft battle damage repair, for instance, quick fixes are being proposed on the basis of static analysis alone. On this basis, perhaps the quickest fix of all is simply to clean up the damage and speedtape the hole. This type of fix could be used on noncritical skin structures. Some of the questions that arise are: What happens when this structure is subjected to a dynamic load environment? Does the presence of the cutout push the structure into a region where resonance could occur, thus leading to damage propagation and possible catastrophic failure? These questions and others are the motivation for the authors' interest in the effects of cutouts in curved composite panels.

Numerous studies examining mode shapes and natural frequencies have been conducted with flat plates. Ashton and Whitney[1] were able to form a solution for symmetric orthotropic plates in which no coupling existed between extension and bending. Rajamani and Prabhakaran[2] investigated the effects of rectangular cutouts on the dynamic response of clamped-clamped flat composite plates. By varying fiber orientation, they were able to show that there is a tendency for the modes to interchange or switch (symmetric to antisymmetric and vice versa) with large cutouts for all modulus ratios except for unidirectional Gr-Ep with a 45-deg fiber orientation.

The purpose of this paper is to extend some of the previous work done on flat plates to panels having curvature in one direction. Another goal is to examine the effects of cutout orientation on the dynamic response, an area that to the best of the authors' knowledge has not been previously addressed.

Approach

A three-part effort was implemented to complete this study. First, holographic interferometry was used to determine the first five natural frequencies and mode shapes for curved retangular Gr-Ep panels having various cutouts. Second, results of a finite-element analysis using STAGS-C1 were compared with those obtained experimentally. Third, having gained confidence in the finite-element results, we examined additional cutout sizes and orientations.

Panel Material and Cutout Geometry

In all, seven panels were constructed. Each was made of Gr-Ep Hercules AS4/3501-6 and were laid up so as to form a quasi-isotropic configuration $[0, -45, +45, 90]_S$. There were eight plies in the layup, each ply having the properties as given in Table 1. The panels were constructed so that [after we allowed for a 2-in. (5.08-cm) clamping surface all around] they were 12 in. (30.48 cm) high, and had a 12-in. (30.48-cm) radius of curvature and 12-in. (30.48-cm) chord length. Measurements taken after panel construction showed that the panel thickness was 0.040 ± 0.001 in. (0.1016 ± 0.0025 cm).

The fabrication and curing of the panels were carried out in standard fashion. The orientations of the 2×4 in. (5.08×10.16 cm) cutouts are based as shown in Fig. 1. The quality of the holes was maintained by employing a curved jig during the cutting process. This jig along with the high-speed carbide-tipped router blade minimized fraying due to cutting vibrations. This setup produced an excellent edge. This was evident by the precision of the cuts made in the panels. The

Received Feb. 10, 1987; revision received Nov. 30, 1987.

*Former Graduate Student, Department of Aeronautics and Astronautics. Member AIAA.
†Assistant Professor, Department of Aeronautics and Astronautics. Member AIAA.
‡Former Graduate Student, Department of Aeronautics and Astronautics.

tolerance was held to ± 0.005 in. (0.0127 cm). Following construction and cutting, each of the panels was painted on one side to enhance the holographic images. The addition of the paint to the surface added less than 0.0001 in. (0.0003 cm) to the thickness and increased the density by only 0.002 lb/in.^{3} (7.225×10^{-8} kg/m^3).

Experimental Setup

Off-the-shelf equipment was used in the experimental setup. A 50-mW helium-neon laser was mounted to an isolation table that had the optical setup as seen in Fig. 2. To expand the laser beam so that the entire panel was illuminated, 20× microscope objectives were used. In order to eliminate the possibility of dust causing refractive fringes, pinhole spatial filters were placed in series with the microscope objectives. Figure 3 shows a schematic of the entire setup.

Real-time holographic interferometry was used to determine the natural frequencies and mode shapes of all the panels tested. For the majority of the testing, two horns were used to excite the panels. When two horns were used, they were either placed inphase or 180 deg out of phase, depending on whether the mode shape of interest was symmetric or antisymmetric. Figure 4 shows the horns positioned in a typical location behind a panel. Except for the relative amplitude of the mode shape, the positioning of the horns at various locations around the concave side of the panels had little effect on the results.

Table 1 Material properties

E_1	18.8×10^6 psi	1.296×10^{11} N/m^2
E_2	1.47×10^6 psi	1.014×10^{10} N/m^2
G_{12}	0.91×10^6 psi	6.274×10^9 N/m^2
ν_{12}	0.2	
ν_{21}	0.022	
ρ	0.055 lb/in.^{3}	1.962×10^{-6} kg/m^3
t	0.005 in.	1.270×10^{-2} cm

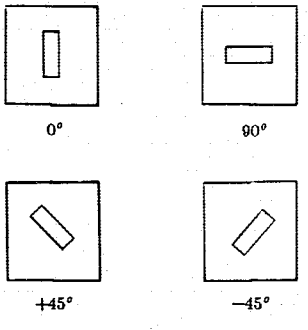

Fig. 1 Cutout orientations.

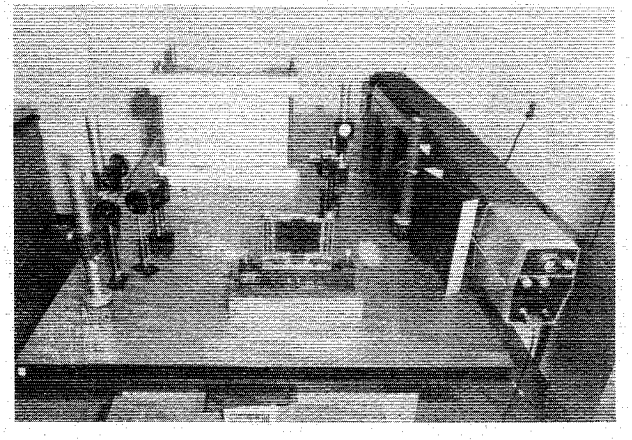

Fig. 2 Experimental setup.

While the panels were being excited by the horns, the presence of subharmonics in a particular mode of interest was precluded by using an optical displacement meter positioned near the surface of the panel to measure the response (see Fig. 5). Figure 6 is a block diagram of the equipment configuration used to check for subharmonics. Lissajous figures observed on an oscilloscope insured that subharmonics were not present.

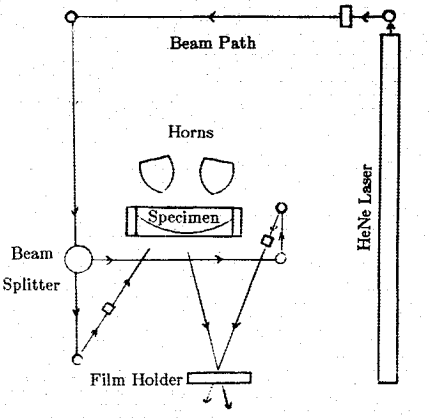

Fig. 3 Schematic of experimental setup.

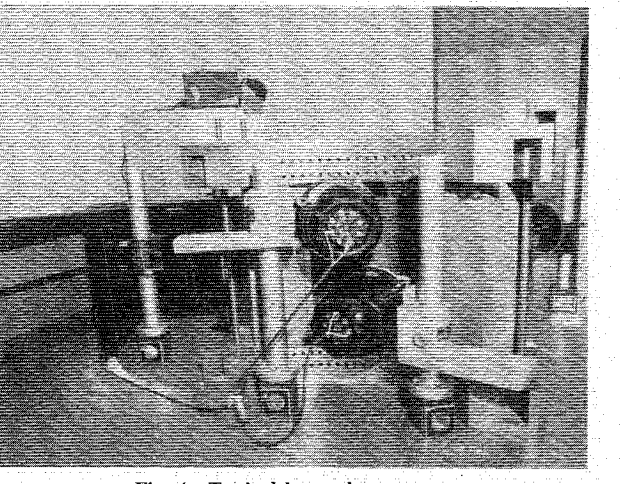

Fig. 4 Typical horn placement.

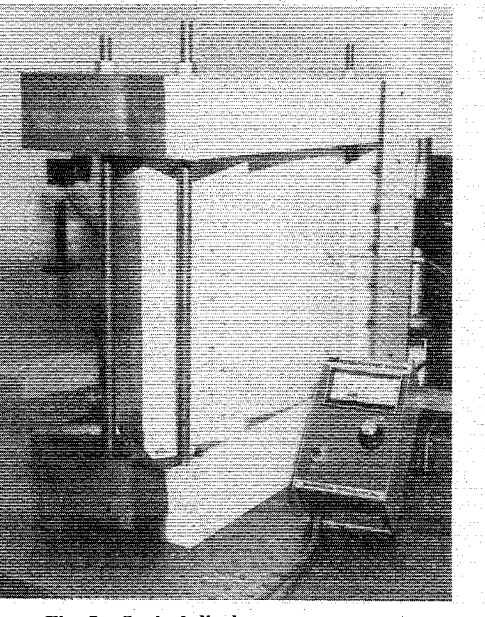

Fig. 5 Optical displacement meter.

The experimental technique used in finding the natural frequencies for all of the panels involved scanning the frequency spectrum from 0 Hz to the fifth natural frequency while observing the fringe patterns on a holographic still photograph of the panel. Whenever a natural frequency was encountered during scanning, a well-defined mode shape appeared on the still photo. The frequency was noted and upward scanning continued until all five natural frequencies were found. The procedure was then reversed and the natural frequencies found by scanning downward. Rarely would the natural frequencies be exactly the same for the upward and downward scans, but the difference was never more than 5 Hz. When time averaged holograms were taken, the frequency was assumed to split these bounds.

Finite-Element Modeling

As was mentioned earlier, the STAGS-C1 program was used for the finite-element modeling of each of the panels. Following a convergence study, it was determined that the most economical arrangement for the accuracy desired was obtained by using a mesh that consisted of the quadrilateral 420 elements[3] discretized such that each element was square with a 1/2-in. (1.27-cm) side. In the case of the ± 45-deg cutouts, the triangular 320 elements were used for refinement around the cutouts. Figure 7 is a typical mesh used for the finite-element analysis.

Results and Discussion

Presentation of the results is in the form of tables showing a comparison of the frequencies for each of the panels obtained experimentally with those obtained by the finite-element

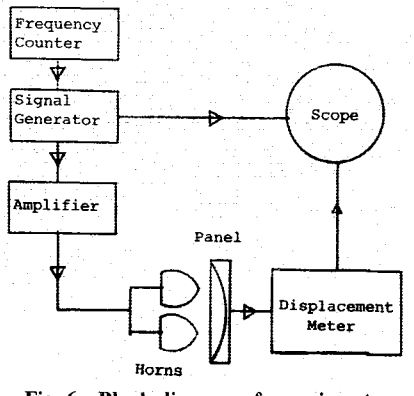

Fig. 6 Block diagram of experiment.

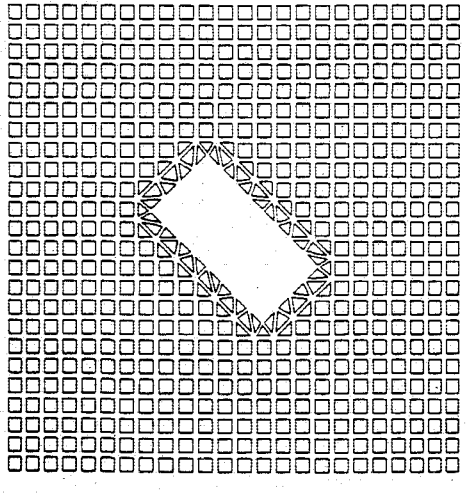

Fig. 7 Typical finite-element model.

Table 2 Solid panel results (natural frequencies in Hz)

Mode	Experiment	STAGS-C1	Error (%)
1	516	506	−1.9
2	527	524	−0.6
3	717	693	−3.2
4	731	703	−3.8
5	840	770	−8.3

Table 3 2 × 2 cutout panel results (natural frequencies in Hz)

Mode	Experiment	STAGS-C1	Error (%)
1	510	505	−1.0
2	546	527	−3.5
3	731[a]	669	−8.5
4	705[a]	691	−2.0
5	756	712	−5.8

[a]Indicates a mode switch.

Table 4 4 × 4 cutout panel results (natural frequencies in Hz)

Mode	Experiment	STAGS-C1	Error (%)
1	477	485	+1.6
2	510	514	+0.7
3	618	612	−1.0
4	691	644	−6.8
5	748	689	−7.9

Table 5 2 × 4 cutout 0-deg panel results (natural frequencies in Hz)

Mode	Experiment	STAGS-C1	Error (%)
1	440	454	+3.2
2	485	536	+10.5
3	577	562	−2.6
4	655	631	−3.7
5	766	703	−8.2

Table 6 2 × 4 cutout 90-deg panel results (natural frequencies in Hz)

Mode	Experiment	STAGS-C1	Error (%)
1	527[a]	514	−2.5
2	496[a]	525	+5.8
3	608	632	+3.9
4	705	675	−4.3
5	731	686	−6.2

[a]Indicates a mode switch.

Table 7 2 × 4 cutout + 45-deg panel results (natural frequencies in Hz)

Mode	Experiment	STAGS-C1	Error (%)
1	513	519	+1.2
2	533	545	+2.3
3	663	651	−1.8
4	700	673	−3.9
5	764	723	−5.4

Table 8 2 × 4 cutout −45-deg panel results (natural frequencies in Hz)

Mode	Experiment	STAGS-C1	Error (%)
1	494	524	+6.1
2	519	551	+6.2
3	608	664	+9.2
4	625	674	+7.8
5	794	744	−6.3

method, and a representative sample of the mode shapes obtained by both methods. Tables 2–8 give the natural frequency comparisons for each of the seven panels tested. The reader will note that for the most part, there is good correlation between the results obtained by experiment with those obtained numerically. The "mode switching" that occurred as indicated in Tables 3 and 6 was an expected phenomenon. Here, mode switching is defined as "when a symmetric or antisymmetric mode shape is expected and the opposite occurs." In Table 6, for instance, the numerical results indicate that the first mode should be antisymmetric and occur at a frequency of 514 Hz, whereas the experimentally observed first mode was found to be symmetric at 496 Hz. This was explored further numerically and the results of the exploration will be presented subsequently.

Figures 8–13 are representative samples of the mode shapes obtained both experimentally and numerically. Again, the agreement between methods is strikingly good. This is an indication that the finite-element method is doing an acceptable job of predicting the results.

Cutout Effects

In this paper, the authors wish to emphasize the effects of cutout orientation on the natural frequencies and mode shapes of the panels. These effects can best be shown graphically in Fig. 14. This figure combines the information presented in tabular form and compares the natural frequencies of the first five modes with the orientation of the cutout. It is interesting to note that for the fundamental mode, there appears to be a significant decrease in the natural frequency for the 0-deg cutout. In order to determine if the dip in the fundamental frequency for that cutout was a minimum, other STAGS-C1 runs were conducted at 27- and 14-deg orientation. The 27-deg orientation was selected because the diagonal of the 2×4 in. (5.08×10.16 cm) rectangle was oriented in the vertical direction (along the 0-deg fiber) and cut through the greatest number of 90-deg fibers. The hypothesis for doing this was that the 90-deg fiber provides the most stiffening properties to the panel in the circumferencial direction and if these fibers are cut, there is a larger corresponding reduction in panel stiffness. There is approximately 5% more net circumferential fiber removed in the 0-deg cutout than the 45-deg cutout. As hypothesized, the 27- and 14-deg cutout orientations had natural frequencies that followed the curves in Fig. 14, thereby supporting the validity that the 0-deg cutout orientation has the lowest fundamental frequency.

As shown in Fig. 14, the numerically derived frequencies were consistently higher than the experimental results for the first two modes. This was probably due to a combination of facts, the panel being modeled using flat elements, the shape functions were not of a high enough order, and the mesh size was not fine enough. The higher modes showed some scatter in the results. This could be attributed to a combination of anomalies in the experimental results due to the clamped boundaries being not fully clamped, or because of variations in the thickness of the panels.

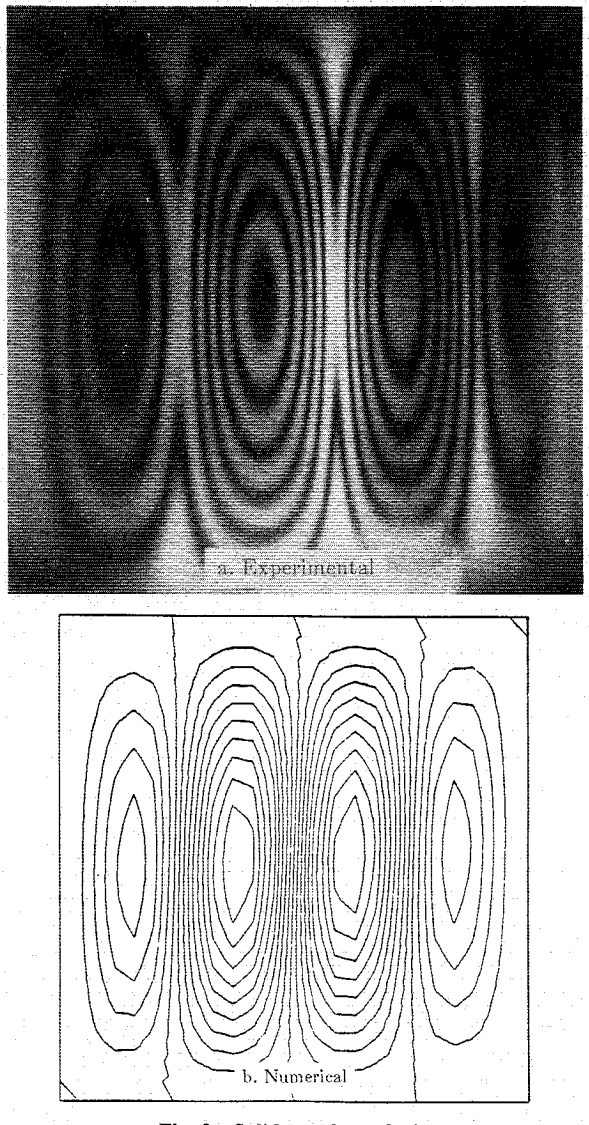

Fig. 8 Solid panel, mode 1.

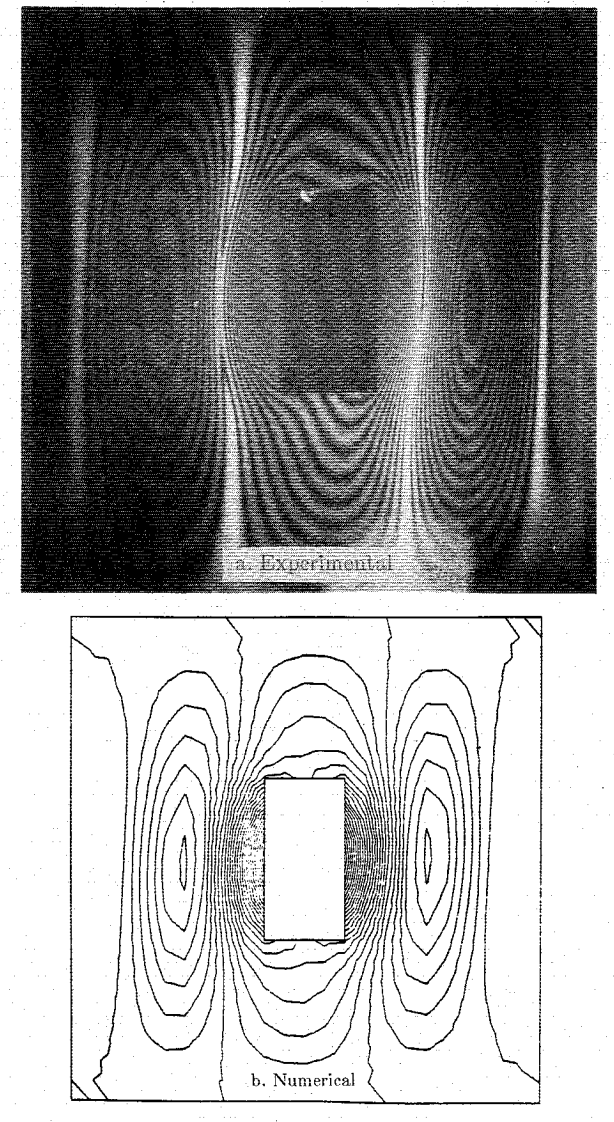

Fig. 9 0-deg cutout, mode 3.

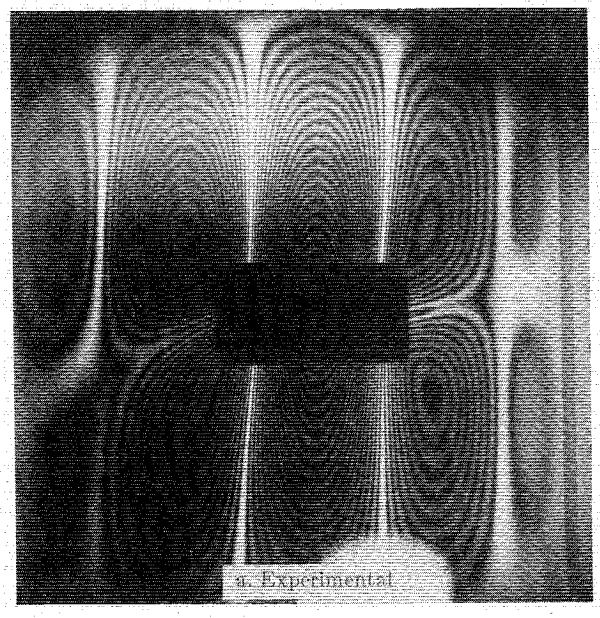

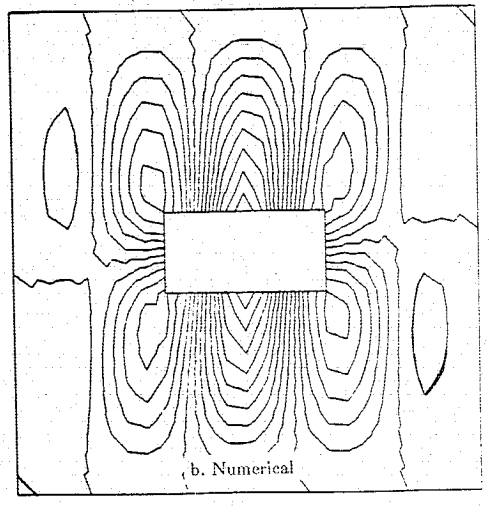

Fig. 10 90-deg cutout, mode 3.

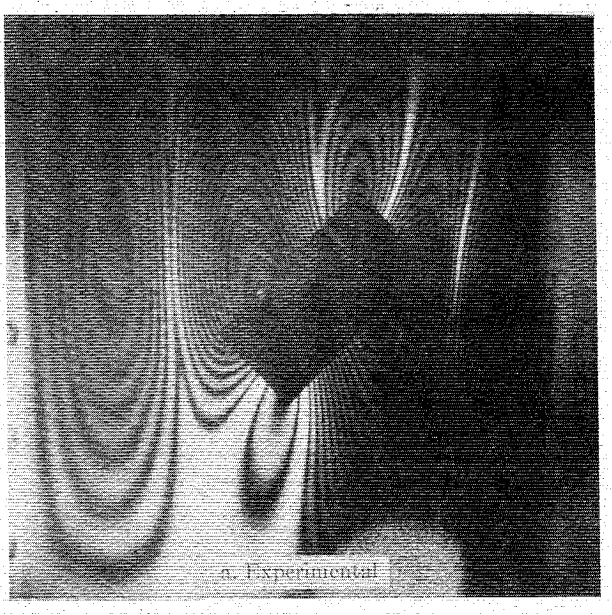

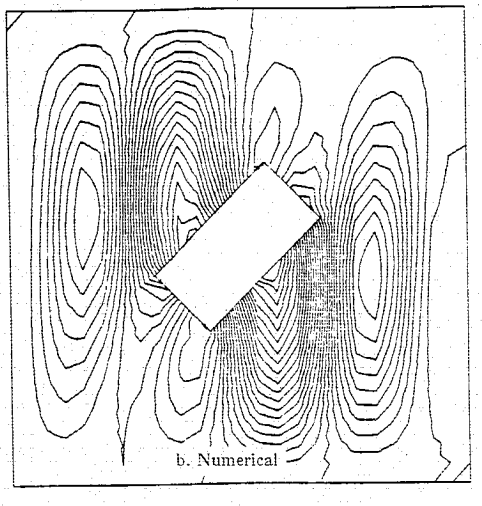

Fig. 11 −45-deg cutout, mode 3.

It is interesting to concentrate one's attention on the numerical results obtained for the first two modes. Although the finite-element mesh for the −45-deg cutout is the mirror image of the mesh for the +45-deg cutout, the results show that first two natural frequencies for these two cases are not the same. At first glance, this would appear to be an illogical observation, and one would be suspicious of the result. Whereas for an isotropic panel, one would indeed obtain the same frequencies for both cases, this is not true for the composite material panel. This is due to the fact that the +45-deg cutout severs a larger number of the −45-deg fibers than +45-deg fibers. The −45-deg cutout severs a larger number of +45-deg fibers. The −45-deg fibers are the outermost 45-deg fibers, thereby having a larger influence on the panel stiffness because of their greater distance from the panel midsurface.

The results shown in Fig. 14 should be of value to the designer. If he were designing a shell with a cutout and the shell were operating near 450 Hz, he would not want to orient the cutout at 0 deg since that would be very close to the fundamental frequency for that orientation. If he has the liberty to do so, he should orient the cutout at a different angle so as to avoid this problem. Another observation that can be made here is that if the designer were interested in placing a cutout in order to cause the least reduction in the natural frequency, he should orient it at the ±45-deg point.

In general, for the 2 × 4 in. (5.08 × 10.16 cm) cutout at any orientation, there was no mode switching. Although for the 90-deg cutout a mode switch was observed experimentally for the fundamental and second natural frequencies, this was most likely an isolated case and a property of that particular panel. Since mode switches were observed in the 2 × 2 in. (5.08 × 5.08 cm) and 4 × 4 in. (10.16 × 10.16 cm) panels, the authors were interested in finding the cutout dimensions at which the mode switch would occur. In order to do this, a numerical study using STAGS-C1 was conducted to determine what critical dimension would cause the phenomena. Although all of the cases run are not shown in this paper, it was found that as the height and width of the cutout were systematically increased, no mode switch occurred until the 3 × 4 in. (7.62 × 10.16 cm) cutout was run. Every cutout larger than this exhibited the switch. The critical dimension appears to be the circumferential dimension.

In order to better understand the mode switch phenomenon, the authors reduced the panel to a 1-DOF spring-mass system or simple harmonic oscillator. An equivalent stiffness for the simple harmonic oscillator was determined from the results obtained for the panel. The mass of the cutout was determined and subtracted from the total mass of the panel. The resultant mass and the derived first and second natural frequencies were used to determine the equivalent spring stiffness

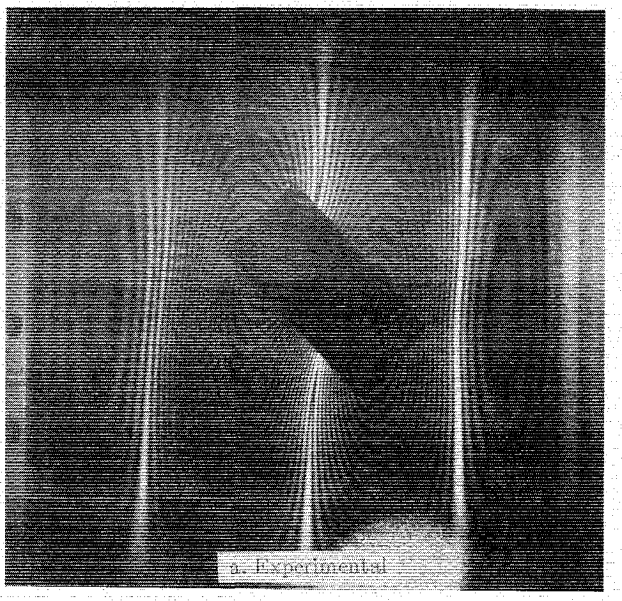

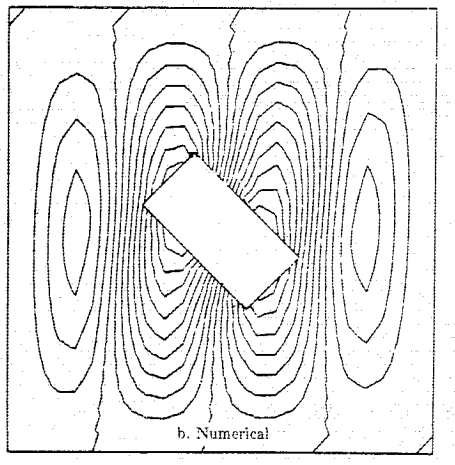

Fig. 12 + 45-deg cutout, mode 1.

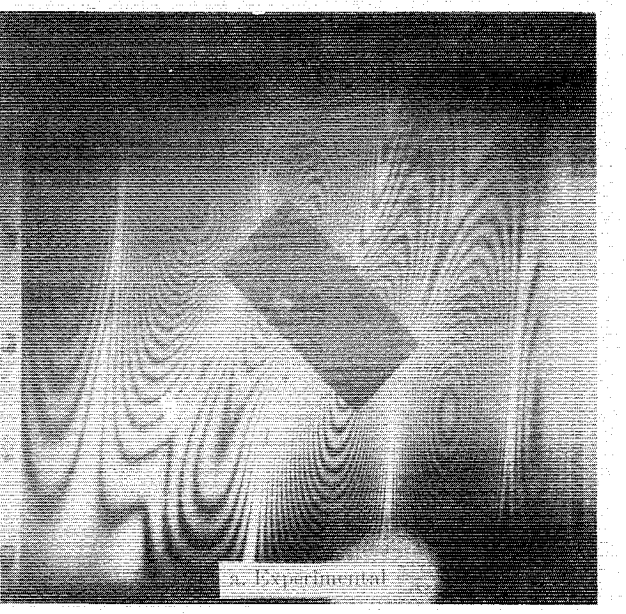

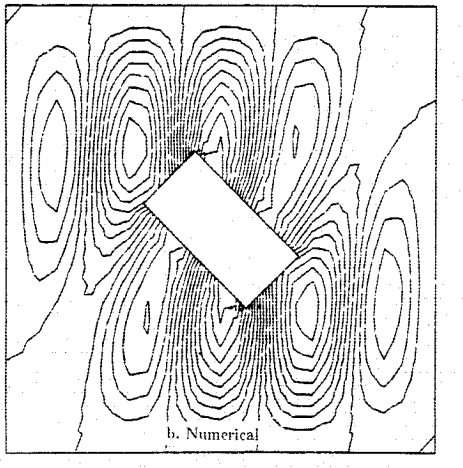

Fig. 13 + 45-deg cutout, mode 5.

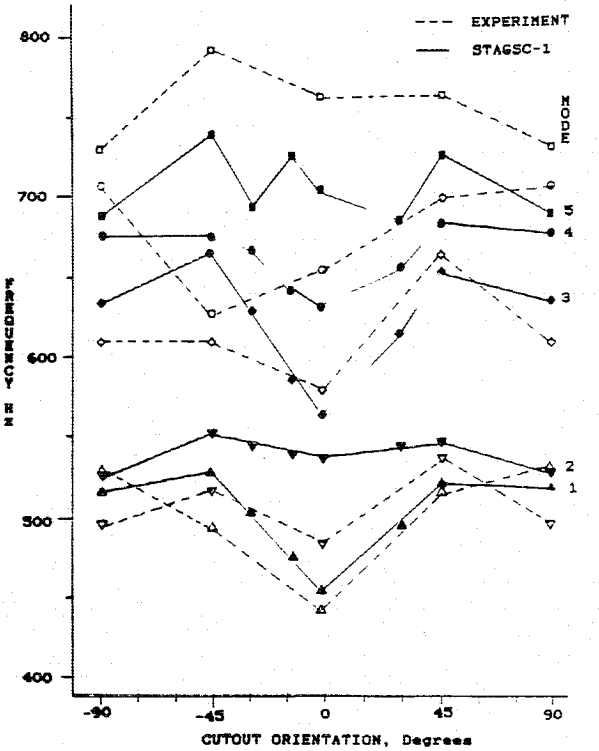

Fig. 14 Cutout orientation vs. frequency.

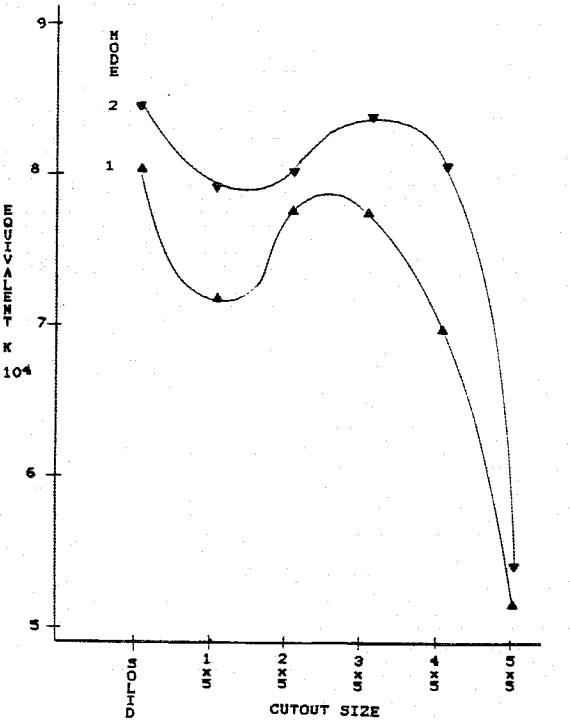

Fig. 15 Equivalent stiffness vs. cutout size.

$$K_{eq} = \omega^2 m \quad (1)$$

Figure 15 shows the results of this simple calculation in which K_{eq} is plotted against the cutout size. In this figure, the 3×5 in. (7.62×12.7 cm) cutout represents a local maximum in the equivalent stiffness and also when the first mode switch would occur for this particular set of data. As the cutout size increases, the equivalent stiffness decreases.

In order to define as closely as possible when the mode switch occurs for this panel, numerical results were generated for cutouts in dimensional increments of 0.33 in. (0.838 cm) near the region of the mode switch. In Fig. 16, the region where the mode switch occurs is evident and shows its dependence on the cutout width and height. In this figure, the *S* stands for a symmetric first mode and *A* an antisymmetric first mode. It is interesting to note that the 2×4 in. (5.08×10.16 cm) cutout seems to border on the mode switch boundary. This fact, coupled with the slight thickness variations present in the panel, could explain why a mode switch occurred experimentally in the 90-deg panel.

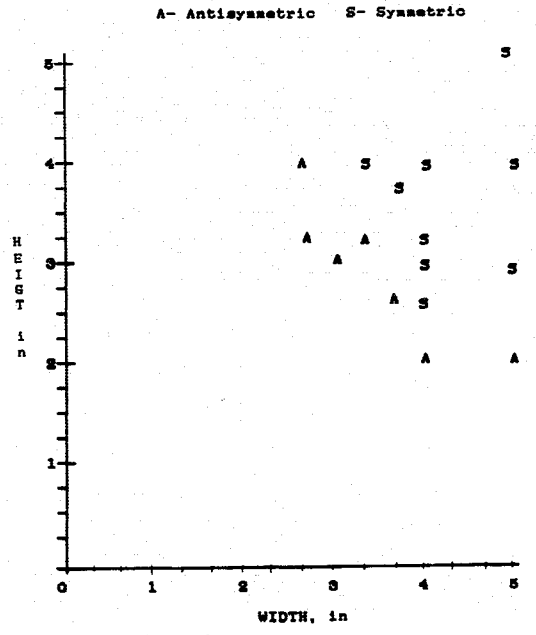

Fig. 16 Mode switch region for mode 1.

Conclusions

In summary, this study investigated the effects of cutout size and orientation on the natural frequencies and mode shapes of curved Gr-Ep composite panels. The study included experimental results obtained by holographic techniques compared with results obtained by the finite-element method. Favorable comparisons between the two methods led to high confidence in the STAGS-C1 finite-element code in predicting the mode shapes and frequencies for the first five modes. As the cutout sizes were increased systematically from a small size [2×2 in. (5.08×5.08 cm)] to the larger size, only minor changes in the mode shapes were observed. This was true in most cases with the exception of a mode "switch" that occurred at a critical dimension of the cutout. This critical dimension is accurately predicted by plotting the equivalent stiffness vs. the cutout size. The critical dimension coincides with a local maximum in this curve. Mode switching appears to be a function of the cutout height and width and not a function of the cutout orientation. This conclusion was supported both in the experimental and numerical studies.

One of the next steps in a continuing project associated with this work is to validate the use of eigenvalue reanalysis of a locally modifed structure using a generalized Rayleigh's method or similar procedure.

References

[1]Ashton, J.E. and Whitney, J.M., *Theory of Laminated Plates*, Technomic Pub. Co., Westport, CT, 1970.

[2]Rajamani, A. and Prabhakaran, R., "Dynamic Response of Composite Plates with Cutouts, Part II, Clamped-Clamped Plates," *Journal of Sound and Vibration*, Vol. 54-4, 1977, pp. 565-576.

[3]Almroth, B.O., Brogan, F.A., and Stanley, G.M., "Structural Analysis of General Shells Volume II," *User Instructions for STAGS-C1, MSC-D673837*, Applied Mechanics Lab., Lockheed Palo Alto Res. Lab., Palo Alto, CA, Jan. 1981.